

Mechanisms of enhanced orbital dia- and paramagnetism: Application to the Rashba semiconductor BiTeI

G. A. H. Schober,^{1,2,3,*} H. Murakawa,⁴ M. S. Bahramy,⁴
R. Arita,^{1,4} Y. Kaneko,⁵ Y. Tokura,^{1,3,4,5} and N. Nagaosa^{1,3,4,†}

¹*Department of Applied Physics, University of Tokyo, Tokyo 113-8656, Japan*

²*Institute for Theoretical Physics, University of Heidelberg, D-69120 Heidelberg, Germany*

³*Cross-Correlated Materials Research Group (CMRG), ASI, RIKEN, Wako 351-0198, Japan*

⁴*Correlated Electron Research Group (CERG), ASI, RIKEN, Wako 351-0198, Japan*

⁵*Multiferroics Project, Exploratory Research for Advanced Technology (ERATO),*

Japan Science and Technology Agency (JST), c/o Department of Applied Physics, University of Tokyo, Tokyo 113-8656, Japan

(Dated: November 4, 2018)

We study the magnetic susceptibility of a layered semiconductor BiTeI with giant Rashba spin splitting both theoretically and experimentally to explore its orbital magnetism. Apart from the core contributions, a large temperature-dependent diamagnetic susceptibility is observed when the Fermi energy E_F is near the crossing point of the Rashba spin-split conduction bands at the time-reversal symmetry point A. On the other hand, when E_F is below this band crossing the susceptibility turns to be paramagnetic. These features are consistent with first-principles calculations, which also predict an enhanced orbital magnetic susceptibility with both positive and negative signs as a function of E_F due to band (anti)crossings. Based on these observations, we propose two mechanisms for the enhanced paramagnetic orbital susceptibility.

PACS numbers: 75.20.Ck, 71.70.Ej, 85.75.-d, 31.15.A-, 71.15.-m

The magnetic susceptibility χ is one of the most fundamental physical quantities, revealing invaluable information about the spin and orbital states of solid materials [1]. The sign of χ , depending sensitively on the mechanism of the magnetization, plays a crucial role in identifying the magnetic properties of bulk systems. From this viewpoint, solid materials are roughly classified into the following three categories [1]: (i) band insulators with weak temperature-independent diamagnetism $\chi < 0$, (ii) metals with temperature-independent Pauli paramagnetic susceptibility $\chi_P > 0$ and temperature-independent Landau diamagnetic susceptibility $\chi_L < 0$ well below the Fermi temperature $T \ll T_F = E_F/k_B$, and (iii) magnetic materials with local moments with strongly temperature-dependent Curie paramagnetic susceptibility $\chi(T) \propto 1/T$ or Curie-Weiss law $\chi(T) \propto 1/(T - T_0)$ corresponding to ferromagnetic ($T_0 > 0$) or antiferromagnetic ($T_0 < 0$) interactions between the magnetic moments. When an electron configuration with $J = 0$ (J : total angular momentum) is realized for a magnetic ion, e.g., in the case of four d -electrons, Larmor diamagnetism and van-Vleck paramagnetism compete to determine the sign of χ .

Usually, the orbital motion of electrons leads to a diamagnetic χ , as in the case of Larmor and Landau diamagnetism. This is due to the cyclotron motion induced by the Lorentz force, which tends to reduce the action of the external magnetic field. When the band gap is reduced or fully closed, this diamagnetic susceptibility is considerably enhanced as in the cases of bismuth [2] and graphene [3]. Especially in graphene, due to the presence of gapless two-dimensional Dirac fermions, χ diverges as $\propto -1/T$ as $T \rightarrow 0$ [3]. Despite this general tendency,

there is no proof that the orbital motion always favors diamagnetism, in particular in the presence of strong spin-orbit interaction (SOI). Hence one cannot exclude the possibility that orbital paramagnetism may be realized in band insulators and metals. So far, however, this possibility has been considered by only a few theoretical studies [4–8]. For example, Vignale [6] showed that a two-dimensional (2D) electron gas in a periodic potential exhibits orbital paramagnetism when the Fermi energy is close to a saddle point of the band structure. Boiko and Rashba [5] predicted orbital magnetism in the Rashba model, for which we will provide the first material realization and its further theoretical analysis below. For band insulators, it has so far been an open question whether orbital paramagnetism can be realized or not.

In this paper, we address the mechanisms of orbital dia- and paramagnetism in semiconductors by studying BiTeI, a narrow-gap polar semiconductor with a non-centrosymmetric layered structure. Due to the polarity of the bulk material and the presence of Bi atoms with large atomic SOI, BiTeI exhibits an extraordinarily large bulk Rashba spin splitting (RSS), astonishingly reaching $\simeq 400$ meV at the bottom of the conduction band as observed in the recent angle-resolved photoemission spectroscopy experiment by Ishizaka *et al.* [9]. Further studies based on optical spectroscopy [10], first-principles calculations and group theoretical analysis [11] have confirmed that this giant RSS is indeed a bulk property of BiTeI, and revealed that in addition to the bottom conduction bands (BCB's), the top valence bands (TVB's) of BiTeI are subject to a comparable RSS. These unique features make BiTeI an ideal medium to explore different

aspects of orbital magnetism in a band insulator system. Below we theoretically predict and experimentally confirm that in BiTeI both an enhanced orbital diamagnetism and an unconventional orbital paramagnetism can be realized by tuning the Fermi energy E_F . This intriguing behavior is shown to be a direct consequence of the RSS.

As described in Refs. 9, 11, BiTeI has a minimum band gap not at the Brillouin zone (BZ) center, but around the hexagonal face center of the BZ, referred to as point A , as shown in Figure 1(a). Due to the strong covalency and ionicity of Bi-Te and Bi-I bonds, respectively, the BCB's are dominated by Bi- $6p$ states, whereas the TVB's are predominantly of Te- $5p$ character with a partial contribution from I- $5p$ states. The huge SOI of Bi accompanied by a strong negative crystal field splitting of TVB's leads BCB's and TVB's to be symmetrically of the same character, and hence to be strongly coupled with each other via a quasi-two-dimensional RSS Hamiltonian. Near point A , this can be described as [11]

$$H_R = \frac{\mathbf{p}^2}{2m^*} + \lambda \mathbf{e}_z \cdot (\mathbf{s} \times \mathbf{p}), \quad (1)$$

where m^* is the effective mass of the carriers, λ is the Rashba parameter, \mathbf{e}_z is the unit vector in z direction, which is the direction of the potential gradient breaking the inversion symmetry, and \mathbf{s} and \mathbf{p} are the spin and momentum operators, respectively. Note in particular the crossing of the BCB's shown in Figure 1(a), which is due to the Kramer's degeneracy at the time-reversal symmetry point A . As fitting parameters, m^* and λ can be tuned [12] such that H_R can properly reproduce the electronic dispersion of BCB's around point A , especially the momentum offset of the conduction band minimum (CBM), $|\mathbf{p}| = \hbar k_0$ with $k_0 = 0.052 \text{ \AA}^{-1}$, and the Rashba energy $E_R = 113 \text{ meV}$, where E_R is the energy of the conduction bands at their crossing point with respect to CBM.

To calculate the orbital magnetic susceptibility χ we employ the Fukuyama formula [13],

$$\chi(T) = \mu_0 \frac{N_A}{N} \frac{e^2 \hbar^2}{2} k_B T \sum_{\ell} \sum_{\mathbf{k}} \text{Tr} [G_{\ell} v_x G_{\ell} v_y G_{\ell} v_x G_{\ell} v_y], \quad (2)$$

where N_A is the Avogadro constant, N the number of carriers, $G_{\ell} = [i\omega_{\ell} + E_F - H]^{-1}$ the one-particle thermal Green's function with Matsubara frequencies $\omega_{\ell} = (2\ell + 1)\pi k_B T$, $\ell \in \mathbb{Z}$, and $v_i = \partial H / \partial k_i$ ($i = x, y, z$) the velocity operators. For the above 2D Rashba model, Figure 1(b) shows the calculated dependence of χ on the Fermi energy E_F . Near the band crossing point, where we take the origin of E_F , an enhanced diamagnetic susceptibility is observed, which diverges as $\chi \propto -1/T$ as in the case of graphene [3]. For $E_F \gg E_R$, χ approaches $-A_{\text{mol}} \mu_0 e^2 / (12\pi m^*)$, which is equivalent to the value of the Landau diamagnetic susceptibility for free electrons with mass m^* in 2D (here A_{mol} is the molar surface area

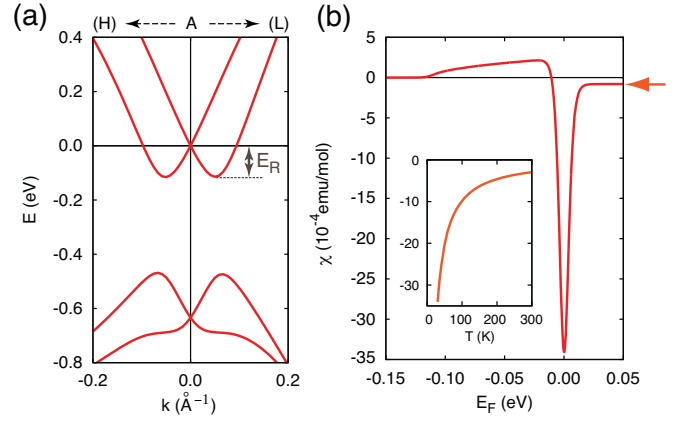


FIG. 1: (Color online) (a) Band dispersion of BiTeI near point A towards the H and L directions. The crossing point of the conduction bands is set at zero energy. (b) Orbital magnetic susceptibility obtained from a 2D Rashba model, which reproduces the dispersion of the BCB's in BiTeI around point A . The main panel shows the Fermi energy dependence of χ at $T = 30 \text{ K}$. The arrow marks the value of the Landau diamagnetic susceptibility for free electrons with mass m^* in 2D (see the related discussion). The inset shows the temperature dependence of the diamagnetic peak value at $E_F = 0$, diverging as $-1/T$.

of one BiTeI layer). In addition, we find the paramagnetic orbital susceptibility when E_F is below the band crossing point, which is a unique feature attributed to the Rashba spin splitting [5].

In the zero temperature limit, by evaluating the frequency sum in the Fukuyama formula we have obtained an analytic formula for the orbital susceptibility of the 2D Rashba model,

$$\chi(T=0) = \mu_0 A_{\text{mol}} \frac{e^2}{m^*} \frac{1}{8\pi k_0} \int_{E_-(k) \leq E_F \leq E_+(k)} \frac{8k^2 - 3k_0^2}{8k^2} dk. \quad (3)$$

Here $k = |\mathbf{k}|$ denotes the radial momentum variable, while the angular integration has already been performed; $E_{\pm}(k) = \hbar^2 k^2 / 2m^* \pm \lambda k$ are the two branches of the Rashba dispersion and $k_0 = m^* \lambda / \hbar^2$ the minimum of the lower branch. For small band fillings, i.e., $E_F \cong -E_R$, the momentum integral is limited to the region where $k \cong k_0$, hence χ is positive and approximately given by

$$\chi(T=0) \cong \mu_0 A_{\text{mol}} \frac{e^2}{m^*} \frac{5}{32\pi} \sqrt{1 + E_F / E_R}. \quad (4)$$

On the other hand, if the Fermi energy is near the band crossing, i.e., $E_F \cong 0$, the region of small k gives the dominant contribution, which gives rise to the negative divergence of the susceptibility as $\chi \propto -1/|E_F|$. [14]

As a supporting argument for the orbital paramagnetism at low band fillings, we have shown in the supplemental material that the energy of the lowest Landau

level of the 2D Rashba model in a perpendicular magnetic field \mathbf{B} is always lower than the minimum energy $-E_R$ in the absence of \mathbf{B} . Accordingly, for sufficiently low filling of the bands, by applying the magnetic field the total energy of the system is lowered, a sign for the occurrence of paramagnetism. Since the Landau-Peierls formula [15], which takes into account only intraband contributions, gives always a negative value for the orbital magnetic susceptibility, the positive χ can be attributed to the interband contributions, which are allowed due to the RSS of BCB's. Also note that this behavior is different from that in the 2D Dirac model describing graphene, which shows only a diamagnetic orbital susceptibility.

To further corroborate these results as well as to explore the effects of all energy bands, we have performed a detailed analysis based on first-principles density functional theory (DFT). The orbital magnetic susceptibility of BiTeI has been computed using the Fukuyama formula (2), with the velocity operator v_i ($i = x, y, z$) represented in matrix form as

$$v_{i,nm} = \langle n | v_i(\mathbf{k}) | m \rangle = \frac{1}{\hbar} \left\langle n \left| \frac{\partial H(\mathbf{k})}{\partial k_i} \right| m \right\rangle, \quad (5)$$

where $|n\rangle$ corresponds to the n th eigenstate of $H(\mathbf{k})$. The numerical computation of $v_{i,nm}$ has been done using the approach of Ref. 16, whereby $H(\mathbf{k})$ is described in the basis of so-called maximally localized Wannier functions (MLWF's) [17]. To fully take into account the contributions of all possible energy states, a set of 18 MLWF's, spanning the 12 highest valence bands and 6 lowest conduction bands, has been generated with the WANNIER90 code [18] by postprocessing [19] the relativistic DFT calculations, initially done using Perdew-Burke-Ernzerhof exchange-correlation functional [20] and the augmented plane wave plus local orbitals method as implemented in the WIEN2K package [21]. For these calculations, the muffin tin radii are set to $R_{MT} = 2.5$ Bohr for all the atoms and the maximum modulus for the reciprocal vectors K_{max} is chosen such that $R_{MT}K_{max} = 7.0$. The BZ is sampled using a $20 \times 20 \times 20$ k-mesh and a full structural optimization is performed until the magnitude of force on each ion is less than 0.1 mRy/Bohr (see Ref. 11 for more details). For the evaluation of the momentum integral in Eq. (2) we have used a $500 \times 500 \times 50$ k-mesh to sample BZ. We have also calculated the Pauli paramagnetic susceptibility χ_P , leaving the orbital degree of freedom unaffected. Namely we have added only the Zeeman coupling $-\mu_B \boldsymbol{\sigma} \cdot \mathbf{B}$ to the Hamiltonian and calculated the spin magnetization to obtain χ_P . However, the contribution of χ_P is much smaller than the orbital χ as described below.

Figure 2 shows the E_F dependence of $\chi + \chi_P$ obtained by the first-principles calculations for BiTeI taking into account the dispersion along k_z direction, where the origin of E_F is taken at the crossing point of BCB's at point A. The Pauli contribution is an order of magni-

tude smaller than the orbital χ , at least in the considered range of $-0.15 \text{ eV} \leq E_F \leq 0.15 \text{ eV}$. This is due to the small effective mass of BCB carriers within the hexagonal face of the BZ (hereafter referred to as ab plane), $m^* \simeq 0.2m$ [10]. This is analogous to the case of bismuth [2] and can be understood by considering a spin-degenerate two-dimensional parabolic band $E = \hbar^2 k^2 / (2m^*)$. Then the orbital and Pauli susceptibility are given by $\chi = -(1/3)\mu_0 N_A \mu_B^{*2} / E_F$ and $\chi_P = \mu_0 N_A \mu_B^2 / E_F$, respectively, where $\mu_B^* = e\hbar / (2m^*)$, $\mu_B = e\hbar / (2m)$, and $E_F = \hbar^2 k_F^2 / (2m^*)$ with the Fermi wave vector k_F . Since m^* appears in E_F , but not in the spin-interaction term, i.e. in μ_B , it turns out that $\chi_P = -3(m^*/m)^2 \chi \simeq -0.1\chi$. Therefore we can neglect χ_P and focus on χ below.

For \mathbf{B} parallel to \mathbf{e}_z , near the band crossing point a large temperature-dependent diamagnetic susceptibility is observed, while the susceptibility turns to be paramagnetic and temperature-independent when E_F is away from it. In contrast, if \mathbf{B} is applied perpendicular to the z direction, χ is found to be always positive and almost insensitive to E_F . The calculated results are in good agreement with the experiment, as shown in Figure 2.

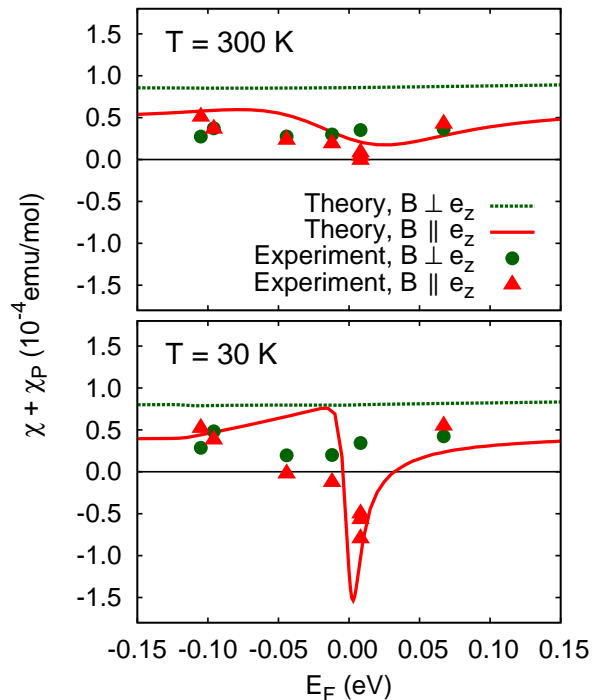


FIG. 2: (Color online) Magnetic susceptibility of BiTeI as a function of Fermi energy E_F , at two temperatures $T = 300 \text{ K}$ (upper panel) and $T = 30 \text{ K}$ (lower panel). Solid lines represent the calculated susceptibility including the Pauli contribution, and points show the corresponding experimental data after subtracting the core contributions. $E_F = 0$ corresponds to the crossing point of the Rashba-split conduction bands at point A.

For the experimental measurement of χ , single crystals of BiTeI with various charge carrier densities were grown by a Bridgman method or chemical vapor transport. The obtained crystals have cleaved (001) planes. The charge carrier density n of each sample was determined by the Hall resistivity measurement, and the corresponding Fermi energy E_F was deduced from the calculated relationship between n and E_F in the 18-band tight-binding model, as shown in Figure 3(a) of Ref. 10. The magnetization measurement was performed with use of the vibrating-sample magnetometer. The sample holder for this was made of a plastic straw tube, whose tiny diamagnetic signal was accurately subtracted.

To extract the orbital magnetic susceptibility from the experimental data, one needs to subtract the Larmor susceptibility χ_L originating from the individual ionic cores in BiTeI. Since in this material the ionic states of Bi, Te and I ions are $3+$, $2-$ and $1-$, respectively, one can assume that they all have closed shell ionic configurations. Accordingly, for each ion χ_L can be easily estimated as [1], $\chi_L = -\mu_0 N_A (e^2/6m) \sum_{i=n,l,j} Z_i \langle r^2 \rangle_i$, where Z_i is the number of electrons occupying state $i = \{n, l, j\}$. Performing a set of all-electron DFT calculations using the LDA1.X program [22], the spread functions $\langle r^2 \rangle_i$ have been individually calculated for all the occupied states of Bi^{3+} , Te^{2-} and I^{1-} (see Table 1 in the supplemental material). Based on these calculations, the respective χ_L of Bi^{3+} , Te^{2-} and I^{1-} are found to be -32.5 , -23.3 and -21.1 (all in units of 10^{-6} emu/mol). We have accordingly subtracted these values from our experimental data to deduce the orbital magnetic susceptibility.

In Figure 3, we show the temperature dependence of the orbital magnetic susceptibility for $\mathbf{B} \parallel \mathbf{e}_z$ at two characteristic Fermi energies, one near the band crossing point ($E_F = 0$) and the other away from it ($E_F \simeq 70$ meV). In the first case, a strong temperature dependence and sign change of χ from paramagnetism to diamagnetism is observed as the temperature is lowered, while in the latter case the susceptibility remains paramagnetic and almost independent of temperature. This behavior is clearly understood in terms of the temperature-dependent enhanced diamagnetic contribution near $E_F = 0$, which adds to the almost temperature-independent paramagnetic interband contribution. All these features are in excellent agreement with the experimental curves measured at two different samples with corresponding carrier densities, as shown in Fig 3.

Up to now, we have focused on the experimentally accessible region -0.15 eV $< E_F < 0.15$ eV. It is of interest to study χ in an extended region to reveal the mechanism of the enhanced orbital magnetism. Figure 4(a) shows the calculated orbital magnetic susceptibility as a function of E_F over the whole energy range of the 18-band model at $T = 300$ K. Large positive and negative values are observed, which are even further enhanced if we consider only the contribution from the ab plane of the BZ

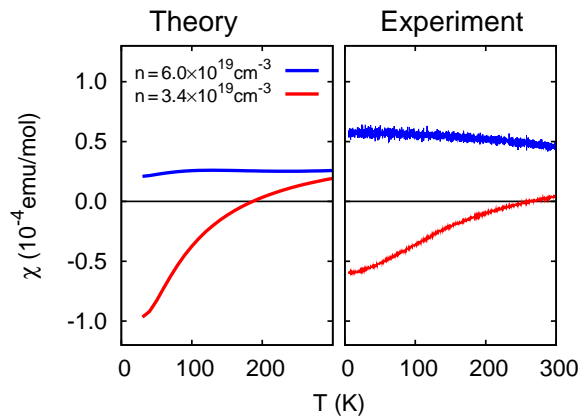


FIG. 3: (Color online) Temperature dependence of the orbital magnetic susceptibility of BiTeI for $\mathbf{B} \parallel \mathbf{e}_z$, obtained theoretically (left panel) and experimentally (right panel) at two characteristic carrier densities. For $n = 3.4 \times 10^{19} \text{cm}^{-3}$ the Fermi energy E_F is close to the band crossing point, whereas for $n = 6.0 \times 10^{19} \text{cm}^{-3}$ it is $\simeq 70$ meV above it.

as in Figure 4(b). It turns out that these large dia- and paramagnetic peaks are caused by (anti)crossings in the band structure of BiTeI, which can be described as 2D tilted Dirac cones. A detailed discussion of the appearance of such tilted Dirac cones in the band structure of BiTeI and their correspondence to the observed dia- and paramagnetic peaks in Figure 4 is given in the supplemental material. There we also provide a simple model which generically describes the dispersion of tilted band crossings and explains the diverging paramagnetic orbital susceptibility as the temperature T goes to zero.

In summary, we have studied the orbital magnetism focusing on its enhancement due to interband effects. As a concrete example we have considered BiTeI with its giant Rashba splitting to see how the spin-orbit interaction affects the orbital magnetism. In addition to the temperature-dependent large diamagnetic susceptibility near the band crossing point analogous to graphene, we have found two mechanisms for the enhanced orbital *paramagnetism*. One is the Rashba splitting with the Fermi energy below the band crossing, and the other is the tilted band crossing.

This research is supported by MEXT Grand-in-Aid No. 20740167, 19048008, 19048015, and 21244053, Strategic International Cooperative Program (Joint Research Type) from Japan Science and Technology Agency, and by the Japan Society for the Promotion of Science (JSPS) through its ‘‘Funding Program for World-Leading Innovative R & D on Science and Technology (FIRST Program)’’. G. A. H. S. acknowledges support from MEXT and DAAD.

- * Electronic address: g.schober@thphys.uni-heidelberg.de
 † Electronic address: nagaosa@ap.t.u-tokyo.ac.jp
- [1] N. W. Ashcroft and N. D. Mermin, *Solid State Physics* (W.B. Saunders Company, 1976).
 [2] W. Nolting and A. Ramakanth, *Quantum Theory of Magnetism* (Springer, 2009); H. Fukuyama and R. Kubo, *J. Phys. Soc. Jpn.* **28**, 570 (1970).
 [3] A. H. Castro Neto, F. Guinea, N. M. R. Peres, K. S. Novoselov, and A. K. Geim, *Rev. Mod. Phys.* **81**, 109 (2009).
 [4] R. Kubo and Y. Obata, *J. Phys. Soc. Jpn.* **11**, 547 (1956).
 [5] I. I. Boiko and E. I. Rashba, *Sov. Phys. Solid State* **2**, 1692 (1960).
 [6] G. Vignale, *Phys. Rev. Lett.* **67**, 358 (1991).
 [7] C. Bruder and Y. Imry, *Phys. Rev. Lett.* **80**, 5782 (1998).
 [8] A. Principi, M. Polini, G. Vignale, and M. I. Katsnelson, *Phys. Rev. Lett.* **104**, 225503 (2010).
 [9] K. Ishizaka *et al.*, *Nature Mater.* **10**, 521 (2011).
 [10] J. S. Lee *et al.*, *Phys. Rev. Lett.* **107**, 117401 (2011).
 [11] M. S. Bahramy, R. Arita, and N. Nagaosa, *Phys. Rev. B* **84**, 041202(R) (2011).
 [12] In our 2D model, m^* and λ are set to $0.09m$ (m : electron

mass) and 4.3 eV\AA , respectively.

- [13] H. Fukuyama, *Prog. Theor. Phys.* **45**, 704 (1971).
 [14] We have confirmed numerically that the contribution from the outer two bands, i.e., $k > k_0$, is a minor part of χ compared with the inner ones ($k < k_0$), see Figure S1 in the supplemental material.
 [15] L. D. Landau, *Z. Phys.* **64**, 629 (1930); R. Peierls, *Z. Phys.* **80**, 763 (1933).
 [16] X. Wang, J. R. Yates, I. Souza, and D. Vanderbilt, *Phys. Rev. B* **74**, 195118 (2006).
 [17] N. Marzari and D. Vanderbilt, *Phys. Rev. B* **56**, 12847 (1997); I. Souza, N. Marzari, and D. Vanderbilt, *Phys. Rev. B* **65**, 035109 (2001).
 [18] A. A. Mostofi *et al.*, *Comput. Phys. Commun.* **178**, 685 (2008).
 [19] J. Kunes *et al.*, *Comput. Phys. Commun.* **181**, 1888 (2010).
 [20] J. P. Perdew, K. Burke, and M. Ernzerhof, *Phys. Rev. Lett.* **77**, 3865 (1996).
 [21] P. Blaha *et al.*, WIEN2K package: <http://www.wien2k.at>.
 [22] LDA1X is a utility code implemented in the program package QANTUMESPRESSO, which is freely available at: <http://www.quantum-espresso.org/>.

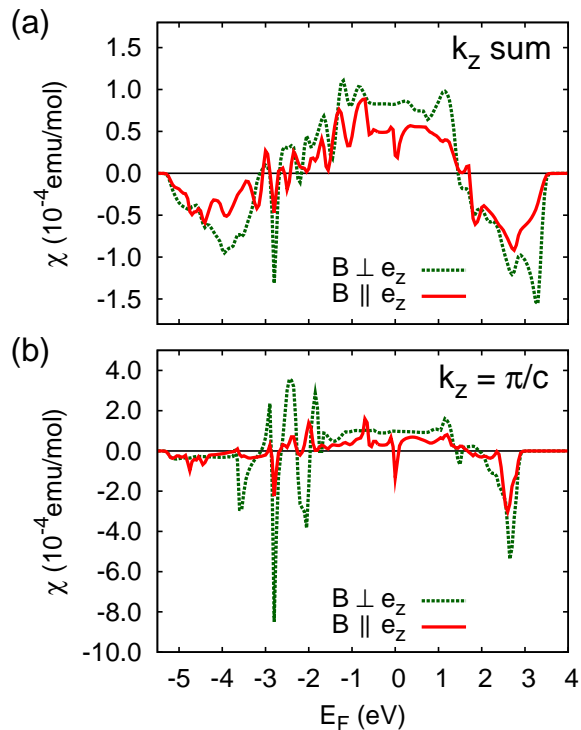


FIG. 4: (Color online) Theoretical results for the orbital magnetic susceptibility in the entire energy range of the 18-band model of BiTeI at $T = 300 \text{ K}$. For (a) we have performed in Eq. (2) the \mathbf{k} integral over the whole three-dimensional Brillouin zone, whereas for (b) we have calculated only the contribution from the ab plane, i.e., we have assumed the integrand to be independent of k_z and taken only the value at $k_z = \pi/c$.